RESEARCH

Profiling analysis of long non-coding RNA and mRNA in parathyroid carcinoma

Xiang Zhang, Ya Hu, Mengyi Wang, Ronghua Zhang, PeiPei Wang, Ming Cui, Zhe Su, Xiang Gao, Quan Liao and **Yupei Zhao**

Department of General Surgery, Peking Union Medical College Hospital, Chinese Academy of Medical Sciences & Peking Union Medical College, Beijing, China

Correspondence should be addressed to Q Liao or Y Zhao: lqpumc@126.com or zhao8028@263.net

Abstract

Parathyroid carcinoma (PCa) is a rare endocrine neoplasia that typically has unfavourable outcomes. The contribution of long non-coding RNAs (lncRNAs) to the development of malignant and benign parathyroid tumours remains largely unknown. In this study, we explored transcriptomic profiling of lncRNA and mRNA expression in 6 PCa, 6 parathyroid adenoma (PAd) and 4 normal parathyroid (PaN) tissues. In total, 2641 lncRNA transcripts and 2165 mRNA transcripts were differentially expressed between PCa and PAd. Enrichment analysis demonstrated that dysregulated transcripts were involved mainly in the extracellular matrix (ECM)–receptor interaction and energy metabolism pathways. Bioinformatics analysis suggested that ATF3, ID1, FOXM1, EZH2 and MITF may be crucial to parathyroid carcinogenesis. Series test of cluster analysis segregated differentially expressed lncRNAs and mRNAs into several expression profile models, among which the 'plateau' profile representing components specific to parathyroid carcinogenesis was selected to build a co-expression network. Seven lncRNAs and three mRNAs were selected for quantitative RT-PCR validation in 16 PCa, 41 PAd and 4 PaN samples. Receiver-operator characteristic curves analysis showed that lncRNA PVT1 and GLIS2-AS1 yielded the area under the curve values of 0.871 and 0.860, respectively. Higher hybridization signals were observed in PCa for PVT1 and PAd for GLIS2-AS1. In conclusion, the current evidence indicates that PAd and PCa partially share common signalling molecules and pathways, but have independent transcriptional events. Differentially expressed lncRNAs and mRNAs have intricate interactions and are involved in parathyroid tumourigenesis. The lncRNA PVT1 and GLIS2-AS1 may be new potential markers for the diagnosis of PCa.

Key Words

- long non-coding RNA
- parathyroid carcinoma
- expression profile
- tumourigenesis

Endocrine-Related Cancer (2019) **26**, 163–176

Introduction

Primary hyperparathyroidism (pHPT) is a common endocrine disorder that is typically caused by benign or malignant neoplasia. Parathyroid adenoma (PAd) is the leading cause of pHPT, while parathyroid carcinoma (PCa) is a rare endocrine malignancy with a poor prognosis. It has been reported that the Asian population presents a higher prevalence of PCa (approximately 5% of pHPT cases) than people in western countries (less than 1% of pHPT cases) (Wang *et al*. 2012). Due to a lack of typical clinical characteristics and specific markers for PCa, it is challenging to distinguish between malignant and benign parathyroid lesions, even with histopathologic imaging, unless local invasion or metastasis has occurred (Cardoso *et al*. 2017). *En bloc* resection is currently considered the

https://erc.bioscientifica.com
https://doi.org/10.1530/ERC-18-0480

best choice for PCa treatment, but the median recurrence time is merely 24 months after the first operation (Xue *et al.* 2016). Clinical practice continues to include repeat surgeries.

As the rarity of PCa, elucidating the mechanisms of its molecular initiation and development is still challenging. A variety of genetic and epigenetic alterations have been reported. SNP array findings support that PCa usually arises *de novo*, instead of developing from a benign adenoma due to the cumulative effect of acquired genetic abnormalities in tumour progression (Vogelstein *et al.* 1989, Costa-Guda *et al.* 2013, Costa-Guda & Arnold 2014). Available data have also identified genetic mutations (*HRPT2*/*CDC73*, *PRUNE2*, etc.), aberrant DNA methylation (APC, HIC1, C19MC, etc.) and dysregulated miRNAs (miR-30b, miR-139, etc.) as contributing factors (Cardoso *et al.* 2017, Silva-Figueroa & Perrier 2018). *CCND1*/*PRAD1* (cyclin D1) and *EZH2* overexpression have been observed in both PCa and PAd (Westin 2016). Common oncogenic events in humans, such as *TP53*, *RB1* and *BRCA2* mutations, appear to be less important than *CDC73* gene mutations in PCa (Adam *et al.* 2010). Epigenetically, parathyroid tumours show active but deregulated global DNA methylation status, and notably, PCa features hypermethylation rather than hypomethylation (Guarnieri *et al.* 2018). miRNA regulation might also be involved in parathyroid tumourigenesis, such as through the Wnt/β-Catenin pathway (Westin 2016). Many overexpressed miRNAs were located at the C19MC genomic cluster, which were identified as characteristics of PCa (Vaira *et al.* 2012). Parathyroid tumours are also thought to have clinical heterogeneity and complex pathogenesis (Farnebo *et al.* 1999, Shi *et al.* 2014). The results derived from whole-exome sequencing, miRNA expression microarray and methylation profiles have shown that PCa has a distinct pathogenesis from that of benign adenoma, but these tumours may share some common early events (Svedlund *et al.* 2012, 2014).

Long non-coding RNAs (lncRNAs), defined as RNA transcripts longer than 200 base pairs, have no coding potential but are active regulators of gene expression. An increasing number of studies have shown that lncRNAs affect tumour biological processes such as chromatin modifications, transcriptional and post-transcriptional gene regulation (Wang & Chang 2011). Dysregulation of lncRNAs is strongly associated with endocrine diseases and cancers (Knoll *et al.* 2015, Bartonicek *et al.* 2016, Schmitt & Chang 2016). Some well-known lncRNAs have been identified in endocrine-related cancers, for example, lncRNA PVT1 in thyroid cancer (Murugan *et al.* 2018) and lncRNA MALAT1 in breast cancer (Peng *et al.* 2018). Moreover, a circulating serum lncRNA was proposed as a potential marker for predicting multiple cancer features (Qi *et al.* 2016, Zhang *et al.* 2016, 2017). To our knowledge, however, there are no published original articles evaluating the role of lncRNAs in the onset and development of PCa and PAd. Therefore, lncRNA expression profiles of PCa and PAd may provide new clues to the mechanisms of parathyroid tumourigenesis.

We examined the expression profile of lncRNAs in PCa and PAd via microarray analyses in a Chinese population. High-throughput data provided us novel perspectives that lncRNAs were differentially expressed, and several key lncRNAs showed potential as candidate markers for PCa. Quantitative RT-PCR (RT-qPCR) assays were performed to confirm the microarray results and for further validation. We then performed integrated analysis of lncRNA and mRNA expression to search for a new key components and pathways of the lncRNAs and protein-coding genes involved in parathyroid tumourigenesis. The expression patterns of differentially expressed lncRNAs and mRNAs related to pathological alteration were investigated using a Series Test of Cluster (STC) analysis. A co-expression network was also constructed to describe the lncRNA–mRNA interactions in PCa and PAd. These results may provide a direction for further exploration into the diagnosis and therapy of parathyroid tumours at the level of transcriptomics.

Methods and materials

Patients and samples

All collected parathyroid tumour samples were obtained in the Peking Union Medical College Hospital (PUMCH) (Beijing, China) during parathyroid tumour excision. This study was approved by the Ethics Committee Board in this hospital, and all individual participants provided written informed consent. A total of 16 PCa, 41 PAd and 4 normal parathyroid gland (PaN) samples were collected for RT-qPCR validation, including those used for microarray detection. PaN tissues were incidentally obtained during surgery from patients with thyroid disease, whose parathyroid function was normal. We randomly selected six PCa, six PAd and four PaN tissues and prepared them for human lncRNA microarray analysis. Histopathological diagnosis of parathyroid lesions was established by two independent pathologists according to the updated WHO guidelines (Lloyd *et al.* 2017). Malignant cases should meet the histopathological criteria mainly including invasion

https://erc.bioscientifica.com
https://doi.org/10.1530/ERC-18-0480

into adjacent structures, capsular and/or extracapsular blood vessels and/or metastasis. The clinical manifestations including recurrence, metastasis and *CDC73* mutation of these malignancies were documented. Specimens from our cohort were stored and administered as described in our previous report (Hu *et al*. 2018). The main clinical characteristics were presented in our previous publication, except for Case No. 4, due to specimen exhaustion (Hu *et al*. 2018). Updated PCa cohort details were presented in Supplementary Table 1 (see section on supplementary data given at the end of this article).

Total RNA extraction and purification

Total RNA was extracted and purified using mirVana miRNA Isolation Kit (Ambion) according to the manufacturer's instructions. RNA quantity was determined using a NanoDrop ND-2000 spectrophotometer (Thermo Scientific), and RNA integrity was assessed using an Agilent Bioanalyzer 2100 (Agilent Technologies).

lncRNA and mRNA microarray profiling

The SBC Human 4 × 180 K lncRNA expression microarray V6.0 (using Agilent SurePrint Technology, designed by Agilent eArray), containing 91,007 probes for lncRNAs and 29,857 probes for coding transcripts, was used in our study. The microarray probes were designed according to authoritative databases, covering GENCODE v21, Ensembl, LNCipedia v3.1, Lncrnadb, Noncoder v4, NCBI and UCSC. In general, total RNA was amplified and labelled with a Low Input Quick Amp WT Labeling Kit (Agilent Technologies), following the manufacturer's protocol. Labelled cRNA was purified using an RNeasy mini kit (Qiagen). Each array was hybridized with 1.65 μg of Cy3-labelled cRNA using a Gene Expression Hybridization Kit (Agilent Technologies) for 17 h at 65°C in a hybridization oven (Agilent Technologies). The processed arrays were finally scanned on an Agilent Microarray Scanner (Agilent Technologies).

Microarray data analysis

Feature Extraction software 10.7 (Agilent Technologies) was used for data extraction, and the raw data were then normalized by Quantile algorithm, limma packages in R. Differentially expressed lncRNAs or mRNAs were identified by fold changes ≥2.0 and $P<0.05$ from the normalized expression levels.

Gene ontology and pathway analysis

Gene ontology (GO) terms (http://www.geneontology.org) describe genes and gene products, including molecular function (MF), cellular component (CC) and biological processes (BP). GO enrichment analysis was performed to evaluate the potential roles of differentially expressed mRNAs. In addition, the Kyoto Encyclopedia of Genes and Genomes (KEGG) database (http://www.kegg.jp/) was used to identify significant pathways for mRNA. Fisher's exact test and P value were applied for detection, and q value was utilized for P value correction.

Ingenuity pathway analysis of differentially expressed mRNA

Ingenuity pathway analysis (IPA) software (www.qiagen.com/ingenuity; Qiagen) was used for network construction and pathway interpretation, which was based on the Ingenuity Knowledge Base (content updated March 2018). Predicted upstream analysis and interaction networks of dysregulated mRNAs were visualized by IPA. The significance of biological relationships among mRNAs and pathways were determined by Fisher's exact test.

STC analysis

STC analysis was performed using normal, adenoma and carcinoma tissues to explore possible changes in lncRNA and mRNA expression patterns in the process of parathyroid pathological alterations. We set PaN, PAd and PCa as distinct stages in parathyroid tumourigenesis and 16 representative significant model profiles independent of the data. STC algorithm and analysis identified the most distinct gene expression profile models (Ramoni *et al*. 2002). A clustering algorithm determined expression tendencies profiling the significantly different genes. Significant profiles with similar changing patterns could be grouped together for comparison and analysis.

lncRNA–mRNA co-expression network

To investigate the relationship among critical lncRNAs and mRNAs in STC profiles, we constructed lncRNA–mRNA co-expression networks using Cytoscape software, version 3.5.1 (http://www.cytoscape.org). A co-expression network was constructed based on the genes enriched in lncRNA–mRNA profiles 7 and 8, which showed the most significant differences. The median expression value of all transcripts was preprocessed. Pearson correlation coefficient and P value between coding RNA or lncRNA

https://erc.bioscientifica.com
https://doi.org/10.1530/ERC-18-0480

Table 1 Primers used for RT-qPCR.

Transcript	**Forward primer** (5′–3′)	**Reverse primer** (5′–3′)
SNORD37	TGATCATTTCTTCACTTTGACCA	AGACGCAGGCTTTCTTCAGT
SIX3-AS1	CCACTCCTCACCACACAACA	AAAGTTTGAGTGCCCTCTGG
MALAT1	TGTCCCTCAAGAGAACACAAGAAG	ACAACTCGCATCACCGGAAT
PVT1	CCAGCACCTGCCTTATCCAA	GAGTCCAGTGATGCTTCCATAGC
lnc-WHSC1L1-12:2	CTGGAGAAGGTGTGTGCTGA	GCATTCAAACTGGTCCCTTC
GLIS2-AS1	TCAACCCCAGGGAGAAACC	CTGAACGTTACGGACGAAGGA
RP11-585P4.6	CACTGAGACTGGGATGGACA	TGGGGAAAAATGCTGGTTTA
TACC3	AGAGAACGAGGAGCTGACCA	TCAGACAGGACAGACAGACG
FAM92A1	TGCAACTTTTGGAAGGCTAA	TGGTGTTCTATGATGAGGCAAC
ANGPTL4	ATGGTGCTGGTGCTGTTGTG	TGTGAGCTCCGCCCAGATA
β-Actin	CTGGAACGGTGAAGGTGACA	CGGCCACATTGTGAACTTTG

were then calculated. For each selected gene pair, the Pearson correlation coefficient was significant with a value of greater than 0.95.

RT-qPCR

Based on their role in the co-expression network and the expression levels in the microarray, seven lncRNAs and three mRNAs were selected as markers for further RT-qPCR validation. Quantitative real-time PCR was performed using SYBR Green assays (ABI, 4368708); β-actin was used as an internal control. Briefly, primers used for each gene were synthesized by Sangon Biotech (Shanghai, China). The primer sequences are listed in Table 1. cDNA was synthesized according to the manufacturer's protocol, and the PCR reaction was performed in a total volume

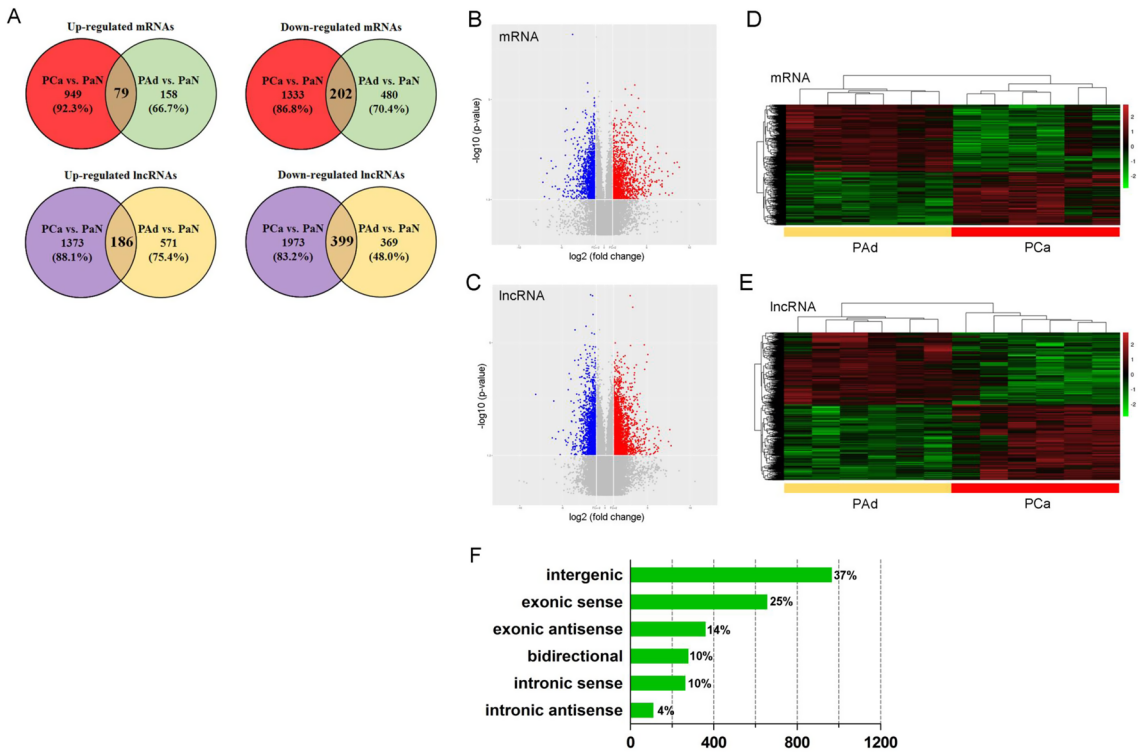

Figure 1
Differentially expressed lncRNAs and mRNAs in parathyroid carcinoma (PCa) and adenoma (PAd) tissues. (A) Venn diagrams present significantly changed profiles of PCa and PAd compared with PaN (FC ≥ 2, $P < 0.05$), showing overlaps between PCa- and PAd-specific genes. (B and C) Volcano plots of mRNA (B) and lncRNA (C) expression variations between PCa and PAd. (D and E) Heat map of 2165 differentially expressed mRNAs (D) and 2641 lncRNAs (E) between PCa and PAd (FC ≥ 2, $P < 0.05$). Red indicates up-regulated transcripts, while green indicates downregulated transcripts. (F) Categories and numbers of 2641 differentially expressed lncRNAs. PAd, parathyroid adenoma; PaN, normal parathyroid glands; PCa, parathyroid carcinoma. A full colour version of this figure is available at https://doi.org/10.1530/ERC-18-0480.

Table 2 Differentially expressed lncRNAs of parathyroid carcinoma compared with adenoma (top 30).

Upregulated			Downregulated		
Accession	*P*-Value	log2 FC	Accession	*P*-Value	log2 FC
NR_046848	0.036627	6.190319	ENST00000548450	0.000496	−8.13029
NR_110331	0.037441	5.916789	lnc-RGS7-3:1	0.022824	−4.49198
NR_033204	0.040371	5.820328	ENST00000568861	0.013139	−4.27656
NR_026880	0.027065	5.801407	lnc-PAM16-2:2	0.000103	−4.19899
lnc-ZNF674-3:2	2.44E-05	5.031564	NR_120631	0.000156	−3.99372
NONHSAT058468	0.006965	5.020488	lnc-RNF217-4:2	0.010095	−3.97738
ENST00000511928	0.003258	4.923444	NONHSAT113817	0.043639	−3.94620
NR_108061	4.3E-05	4.910892	lnc-EPHA1-2:1	0.003713	−3.92554
NR_125823	0.033822	4.668267	lnc-RNF217-4:3	0.003902	−3.88983
NR_108061	7.49E-05	4.661395	lnc-FAM55B-1:1	0.001843	−3.79764
NR_125365	1.18E-05	4.616725	NR_034096	0.001710	−3.62189
ENST00000584683	0.004888	4.616256	lnc-QRFP-2:2	0.002412	−3.58788
ENST00000584807	0.014126	4.53652	lnc-TLR5-1:4	0.046550	−3.55688
lnc-DDB1-2:1	0.000468	4.121762	NR_038939	3.79E-06	−3.51229
ENST00000605056	0.001072	3.869599	lnc-MCMBP-3:1	0.026641	−3.48467
ENST00000519481	0.001014	3.832993	lnc-SLC4A2-2:1	0.044018	−3.44106
lnc-ZNF623-1:1	0.000761	3.822221	NR_040019	0.004074	−3.41198
lnc-SLC22A16-2:1	0.000500	3.773237	lnc-HMOX1-2:2	0.037259	−3.15649
ENST00000447507	0.000633	3.733016	ENST00000458252	0.000788	−3.13470
lnc-CXorf36-1:2	5.32E-05	3.67858	NR_110901	5.41E-05	−3.12691
lnc-AKR1C3-4:1	0.004713	3.664487	lnc-MRP63-5:5	3.68E-05	−3.11861
NR_046848	0.002250	3.634898	NR_125398	0.000511	−3.04554
lnc-MYC-2:22	0.002247	3.563315	ENST00000435112	0.001351	−3.03387
ENST00000625132	0.000717	3.537331	NR_125911	0.003143	−2.98251
lnc-CAND1-2:1	0.000594	3.526152	lnc-GOLGA5-1:1	0.024192	−2.95691
ENST00000608963	0.004527	3.465576	lnc-ST8SIA5-1:2	0.014771	−2.95534
ENST00000432120	6.64E-05	3.446623	ENST00000417792	0.000136	−2.95021
lnc-LHFPL4-5:1	0.005000	3.441390	ENST00000522388	0.003718	−2.95014
NR_125865	0.000114	3.432209	ENST00000610158	0.003485	−2.91175
NR_015422	0.000586	3.360198	lnc-MTRR-7:4	0.000729	−2.90318

FC, fold change.

of 20 µL, including 4 µL of RT buffer (5×), 1 µL of enzyme mix, 1 µL of primer mix and 14 µL of RNA template (0.5 µg) and H_2O. RT-qPCR was conducted on a 7900 HT Sequence Detection System (ABI, USA). The reactions were incubated in a 384-well optical plate (ABI, Cat. #4309849) at 50°C for 2 min and 95°C for 10 min, followed by 40 cycles of 95°C for 15 s and 60°C for 1 min. The classical $2^{-\Delta Ct}$ method was used to calculate the relative amount of lncRNA and mRNA expression.

lncRNA *in situ* hybridization

Two lncRNA markers were selected to be validated in formalin-fixed paraffin-embedded (FFPE) tissues of PCa and PAd. The lncRNA *in situ* hybridization (ISH) procedure was performed according to the manufacturer's instructions. The digoxigenin (DIG)-labelled (5′ and 3′) ISH primers used for lncRNA GLIS2-AS1 and lncRNA PVT1 were as follows: GLIS2-AS1, 5′-DIG-CACTGCA TTGGTTTCTCCCTGGGGTTG-DIG-3′; PVT1, 5′-DIG-CTG ATTTCCGTTACTGCTCACCTGCGA-DIG-3′. The lncRNA probes were synthesized by TSINGKE Biological Technology (Beijing, China). The probe (8 ng/µL) was incubated overnight at 37°C in an incubator. After washing out the hybrids and BSA blocking, the probe was visualized with BCIP/NBT (Boster Bio, USA). The degree of blue staining indicated positive ISH signal intensity. Independent assessment of ISH signals was performed by two doctors who were blinded to the diagnoses and clinical features.

Statistical analyses

Statistical analyses were performed using SPSS, version 23.0 for Windows (IBM). The Kruskal–Wallis test was used to compare the expression of lncRNAs and mRNAs between groups ($P<0.05$ was considered significant). Receiver-operator characteristic curves (ROC) were constructed, and the area under the curve (AUC) was calculated to assess the diagnostic efficiency of the lncRNA markers.

https://erc.bioscientifica.com
https://doi.org/10.1530/ERC-18-0480

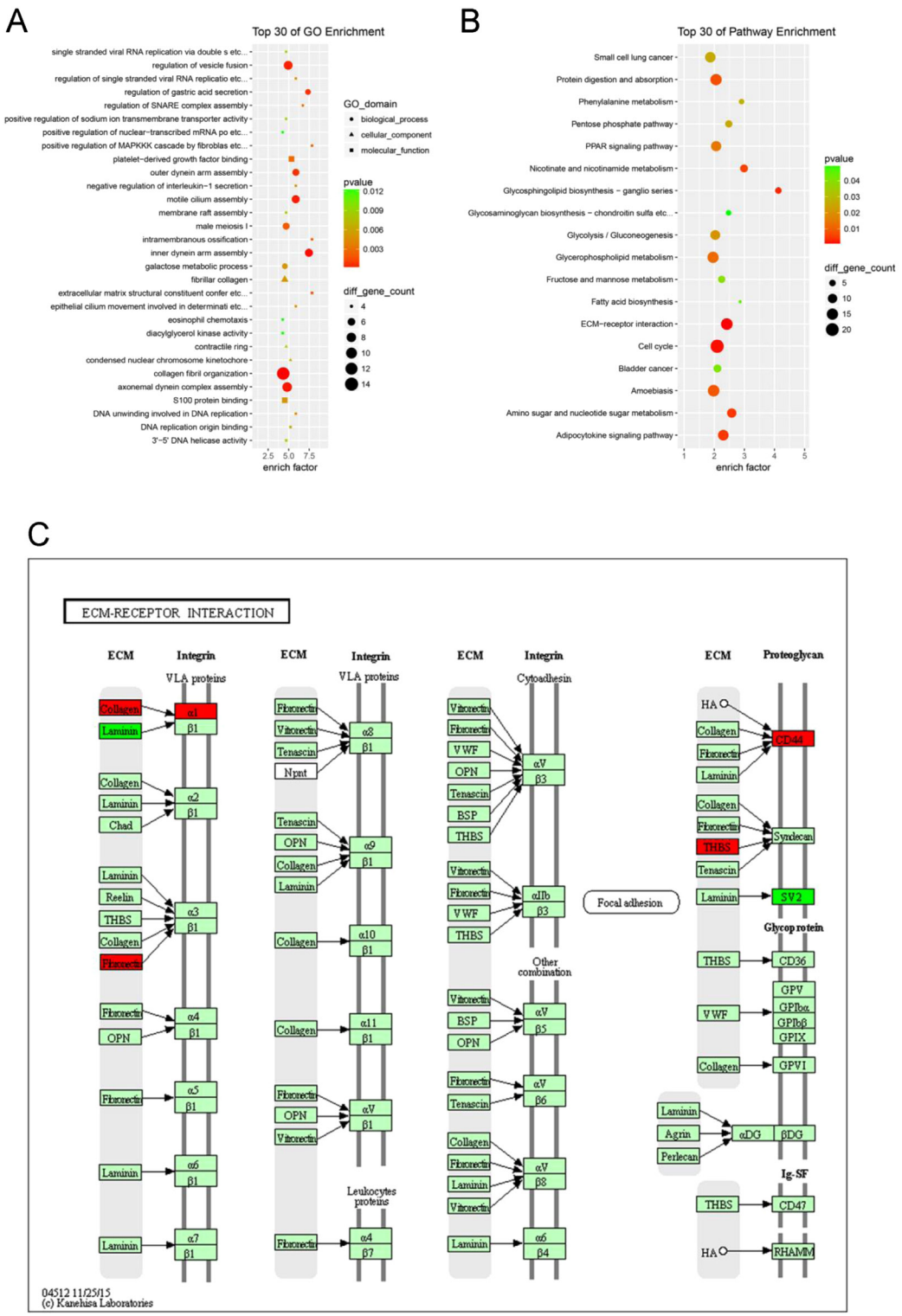

Figure 2

The results of GO and KEGG pathway analysis. (A and B) The horizontal axis represents the enrichment factor, and the vertical axis represents the GO or pathway category. (C) Leading pathway annotation indicates the ECM-receptor interaction pathway. Red marks are associated with upregulated genes, while the nodes in brilliant green indicate down-regulation. Light green indicates no significance. GO, gene ontology; KEGG, Kyoto Encyclopedia of Genes and Genomes.

https://erc.bioscientifica.com
https://doi.org/10.1530/ERC-18-0480

Table 3 Significant KEGG pathways for differentially expressed mRNAs (ranked according to *P*-value).

Pathway	Description	*P*-Value	Enrichment factor
hsa04512	ECM-receptor interaction	0.001181	2.42
hsa04110	Cell cycle	0.001653	2.1
hsa00604	Glycosphingolipid biosynthesis – ganglio series	0.003227	4.13
hsa04920	Adipocytokine signalling pathway	0.004646	2.3
hsa00520	Amino sugar and nucleotide sugar metabolism	0.004743	2.58
hsa00760	Nicotinate and nicotinamide metabolism	0.005981	2.99
hsa04974	Protein digestion and absorption	0.007475	2.06
hsa05146	Amoebiasis	0.008881	1.98
hsa00564	Glycerophospholipid metabolism	0.01223	1.96
hsa03320	PPAR signalling pathway	0.01467	2.06
hsa00010	Glycolysis/gluconeogenesis	0.02053	2.03
hsa00030	Pentose phosphate pathway	0.02491	2.48
hsa05222	Small cell lung cancer	0.0255	1.87
hsa00360	Phenylalanine metabolism	0.02684	2.91
hsa00051	Fructose and mannose metabolism	0.03954	2.25
hsa05219	Bladder cancer	0.04132	2.11
hsa00061	Fatty acid biosynthesis	0.04489	2.86
hsa00532	Glycosaminoglycan biosynthesis – chondroitin sulphate/dermatan sulphate	0.04976	2.48

Results

Differential expression of lncRNAs and mRNAs in PCa and PAd tissues

Using microarray analyses, 2563 mRNA transcripts (1028 upregulated and 1535 down-regulated) and 3931 lncRNA transcripts (1559 upregulated and 2372 downregulated) were differentially expressed between PCa and PaN (PCa vs PaN) (fold change (FC) ≥2, $P<0.05$). Moreover, 919 mRNA transcripts (237 upregulated and 682 downregulated) and 1525 lncRNA transcripts (757 upregulated and 768 downregulated) were aberrantly expressed in the PAd-PaN comparison (PAd vs PaN) (FC ≥2, $P<0.05$) (Fig. 1A).

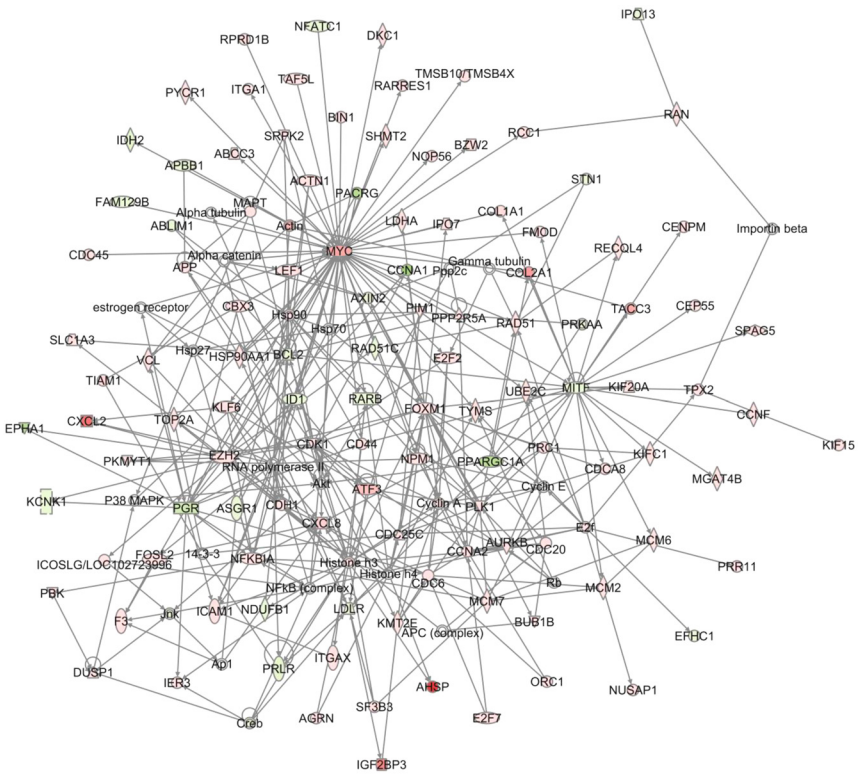

Figure 3
IPA analysis of differentially expressed mRNA between PCa and PAd. One of the most significant networks with 114 focus molecules (score, 96). Upregulated node genes are depicted in red, while downregulated genes are depicted in green. A full colour version of this figure is available at https://doi.org/10.1530/ERC-18-0480.

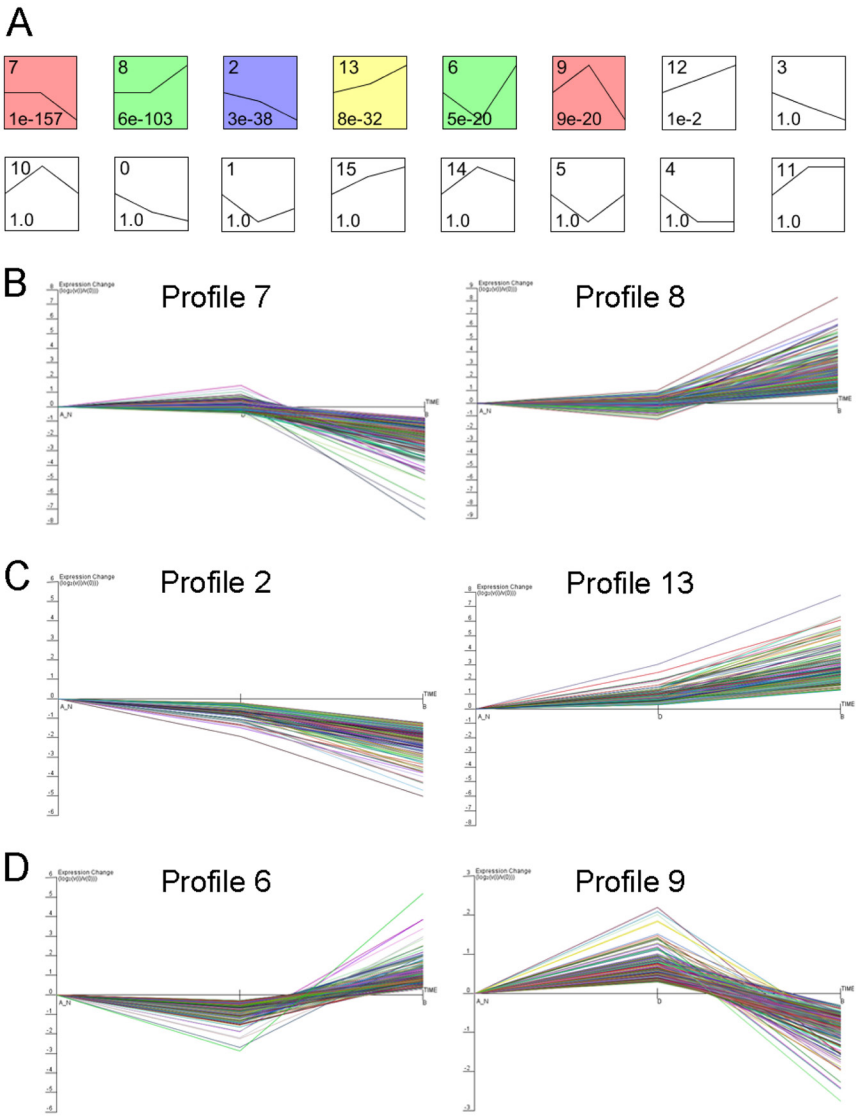

Figure 4
STC analysis of expression profiles of lncRNAs and mRNAs in parathyroid tumours. (A) Each box represents a model expression pattern. The upper number ranging from 0 to 15 marks the mode profile. A total of six significant profiles were identified with $P < 0.05$. (B) Profiles 7 and 8 are the most significant patterns, which were defined as 'plateau' type. (C) Profiles 2 and 13 were defined as 'coherent' type. (D) Expression patterns of profiles 6 and 9 are presented. The vertical axis shows the transcript expression level after Log2 normalized transformation. A_N, normal tissue; B, parathyroid carcinoma; D, parathyroid adenoma. A full colour version of this figure is available at https://doi.org/10.1530/ERC-18-0480.

Volcano plots were used to depict the gene expression variation between PCa and PAd, demonstrating 2641 dysregulated lncRNAs (1350 upregulated and 1291 downregulated) and 957 upregulated mRNAs and 1208 downregulated mRNAs (Fig. 1B, C, D and E). A hierarchical cluster heatmap was used to classify the PCa and PAd groups. The 2641 lncRNAs were classified into six categories: intergenic (37%) and exonic sense (25%) constituted the largest categories; other lncRNAs comprised exonic antisense (14%), bidirectional (10%), intronic sense (10%) and intronic antisense (4%) (Fig. 1F). Table 2 lists the most marked 30 upregulated and downregulated lncRNAs of PCa compared with PAd from our microarray.

Bioinformatics analysis of differentially expressed mRNAs involving malignant and benign parathyroid tumourigenesis

Differentially expressed mRNAs between PCa and PAd underwent GO and KEGG pathway analysis. The GO analysis results revealed a number of biological processes, cellular components and molecular functions that differed between PCa and PAd (Fig. 2A). In the KEGG Pathway analysis, significant KEGG pathways were enriched (Fig. 2B). We ranked the pathway list by *P* value (Table 3). The extracellular matrix (ECM)–receptor interaction was the pathway that most correlated with PCa. In addition, enriched pathways included several metabolism-associated

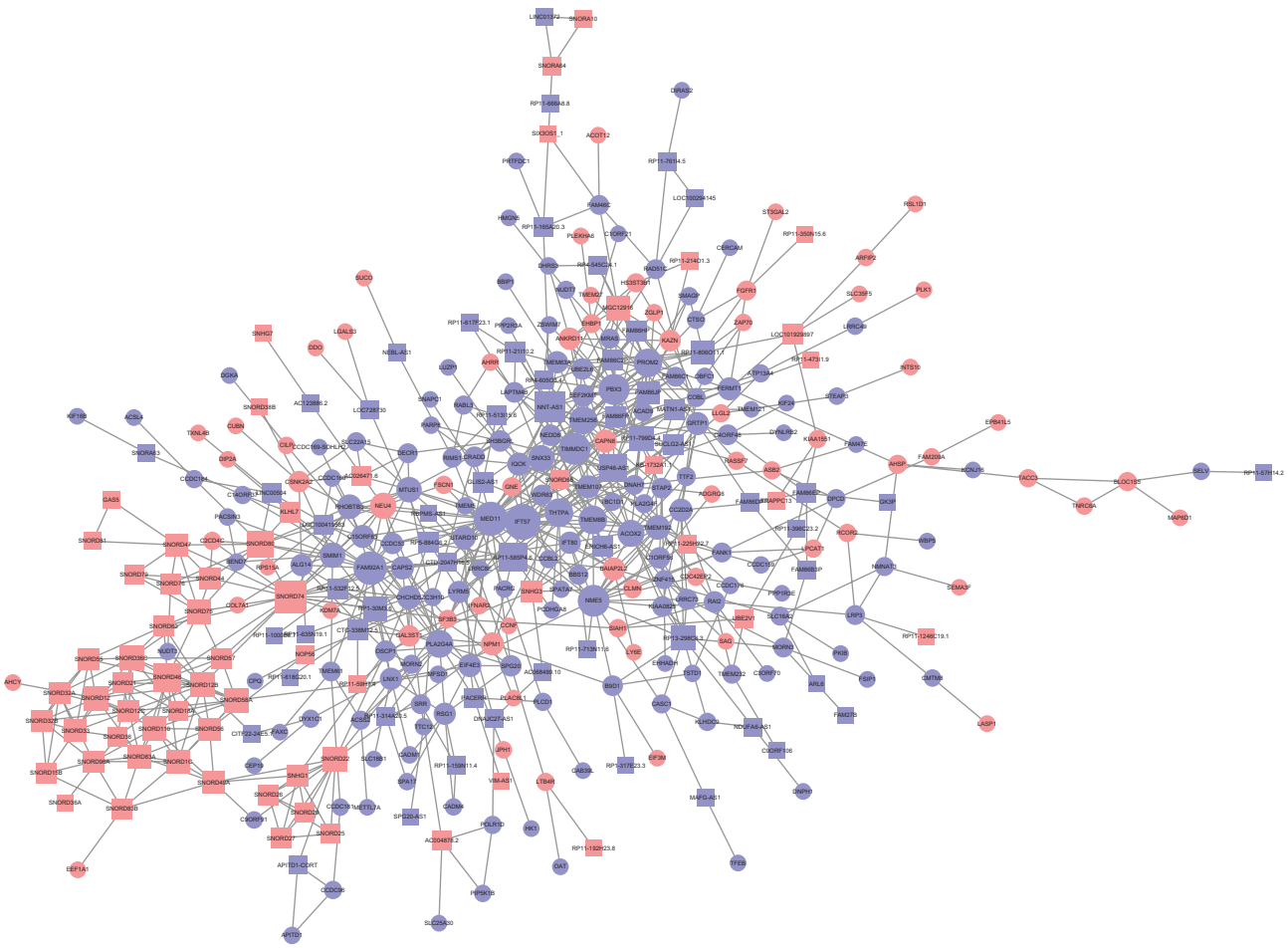

Figure 5
Co-expression network of 'plateau' profile. In the network, continuous lines indicated gene correlations, ellipse nodes represented mRNAs and rectangle nodes represented lncRNAs. Genes in different profiles are shown as different colours (profile 7, violet; profile 8, pink). A degree scoring was used to evaluate hub genes in the network. Values of degree were calculated according to the connection among other genes. Larger size of the nodes indicated higher degree scoring and a more central role of lncRNA or mRNA. A full colour version of this figure is available at https://doi.org/10.1530/ERC-18-0480.

pathways such as the adipocytokine signalling pathway, the PPAR signalling pathway, glycolysis/gluconeogenesis and the pentose phosphate pathway (Fig. 2C).

For the purpose of building more comprehensive knowledge and obtaining a better understanding of the core of PCa regulation and tumour formation, we further launched IPA analysis of the microarray data. Significant biological networks were determined between PCa and PAd. One of the significant networks was marked as 'Cell Cycle, Cell Death and Survival, Cellular Development' (Fig. 3). The other three charts of molecular networks were also produced for PCa–PAd difference (Supplementary Figs 1, 2 and 3). IPA plotted 11 predicted regulatory mechanisms on PCa tumourigenesis according to the consistency score calculation. The predicted mechanisms with the highest scores are shown in Supplementary Fig. 4. We found that ATF3, ID1, FOXM1, EZH2 and MITF were the upstream regulators of crosstalk critical to the development of parathyroid tumours (Supplementary Figs 5, 6, 7, 8 and 9).

STC analysis of lncRNA and mRNA model profiles

We hypothesized that PaN, PAd and PCa gradually develop in an evolutionary model. Expression trends of differentially expressed lncRNAs and mRNAs were assessed by STC calculation. Each profile consisted of a cluster of lncRNAs and mRNAs with similar expression patterns. Sixteen profiles (profiles 0–15) were established representing sixteen expression models, and six significantly different profiles were identified (Fig. 4A).

https://erc.bioscientifica.com
https://doi.org/10.1530/ERC-18-0480

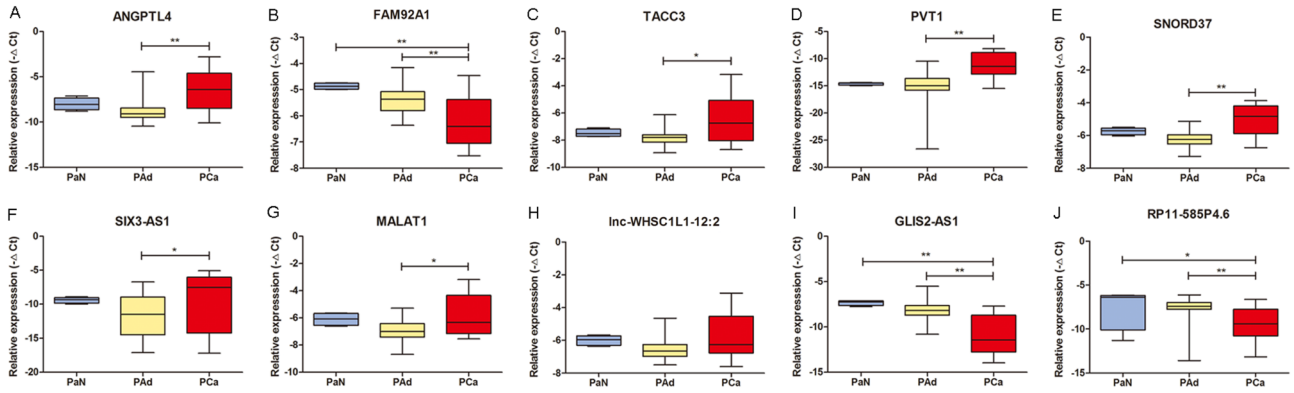

Figure 6
Validation of differentially expressed mRNAs and lncRNAs in PCa and PAd patients. (A, B and C) Selected mRNAs were validated by RT-qPCR. Upregulated (D, E, F, G and H) and downregulated (I and J) candidate lncRNAs were chosen for potential markers. All transcripts were verified in a cohort of PCa ($n = 16$), PAd ($n = 41$) and PaN tissue samples ($n = 4$). $^{*}P < 0.05$, $^{**}P < 0.01$. A full colour version of this figure is available at https://doi.org/10.1530/ERC-18-0480.

The most significant profiles (profiles 7 and 8), indicating a separate entity, were defined as the 'plateau' type (Fig. 4B). Profiles 2 and 13 changed continuously and showed significance and were defined as 'coherent' types (Fig. 4C). Profiles 6 and 9 exhibited markedly different expression patterns and indicate different functions in PCa and PAd (Fig. 4D).

Construction of a co-expression network

The differentially expressed lncRNAs and mRNAs of the 'plateau' profiles were selected as the most significant expression patterns to build the co-expression network. The network in the 'plateau' profile comprised 123 lncRNAs and 221 mRNAs (Fig. 5), processing 344 network nodes and 791 pairs of connections. A complicated association among lncRNAs and mRNAs was indicated in the profiles. The top 30 core nodes are listed in Table 4 with the highest degree scored representing the leading roles in PCa tumourigenesis.

Microarray validation and diagnostic efficiency of lncRNA markers

To validate the results of the microarray, we chose a total of three mRNAs (ANGPTL4, FAM92A1 and TACC3) and seven lncRNAs (GLIS2-AS1, lnc-WHSC1L1-12:2, MALAT1, PVT1, RP11-585P4.6, SIX3-AS1 and SNORD37) transcripts for further RT-qPCR. These lncRNAs were screened as specific candidate markers for PCa. Consequently, Kruskal–Wallis analysis demonstrated that PVT1, SNORD37, SIX3-AS1, MALAT1 were significantly upregulated, and GLIS2-AS1 and RP11-585P4.6 were significantly downregulated in PCa compared with PAd tissues. RT-qPCR results were generally consistent with the microarray data (Fig. 6). Further ROC analysis revealed that lncRNA PVT1 and lncRNA GLIS2-AS1 have a novel diagnostic value between PCa and PAd, with AUC values of 0.871 and 0.860, respectively (Fig. 7 and Table 5). Interestingly, *CDC73*-mutant

Table 4 Top 30 core nodes with the highest degree scoring in the co-expression network.

Transcripts	Degree	Profile	Type
IFT57	25	7	Coding
MED11	23	7	Coding
FAM92A1	22	7	Coding
NME5	20	7	Coding
SNORD74	20	8	Non-coding
TIMMDC1	20	7	Coding
PBX3	19	7	Coding
NNT-AS1	18	7	Non-coding
PROM2	16	7	Coding
RP11-585P4.6	16	7	Non-coding
THTPA	16	7	Coding
TMEM8B	16	7	Coding
PLA2G4A	15	7	Coding
SNORD46	15	8	Non-coding
TMEM256	15	7	Coding
ACOX2	14	7	Coding
USP46-AS1	14	7	Non-coding
NEU4	13	8	Coding
SNORD80	13	8	Non-coding
SNX33	13	7	Coding
MTUS1	12	7	Coding
SMIM1	12	7	Coding
RHOBTB3	11	7	Coding
RP11-799D4.4	11	7	Non-coding
RP13-298C8.3	11	7	Non-coding
SNORD22	11	8	Non-coding
SNORD36C	11	8	Non-coding
TMEM192	11	7	Coding
CHCHD5	10	7	Coding
MGC12916	10	8	Non-coding

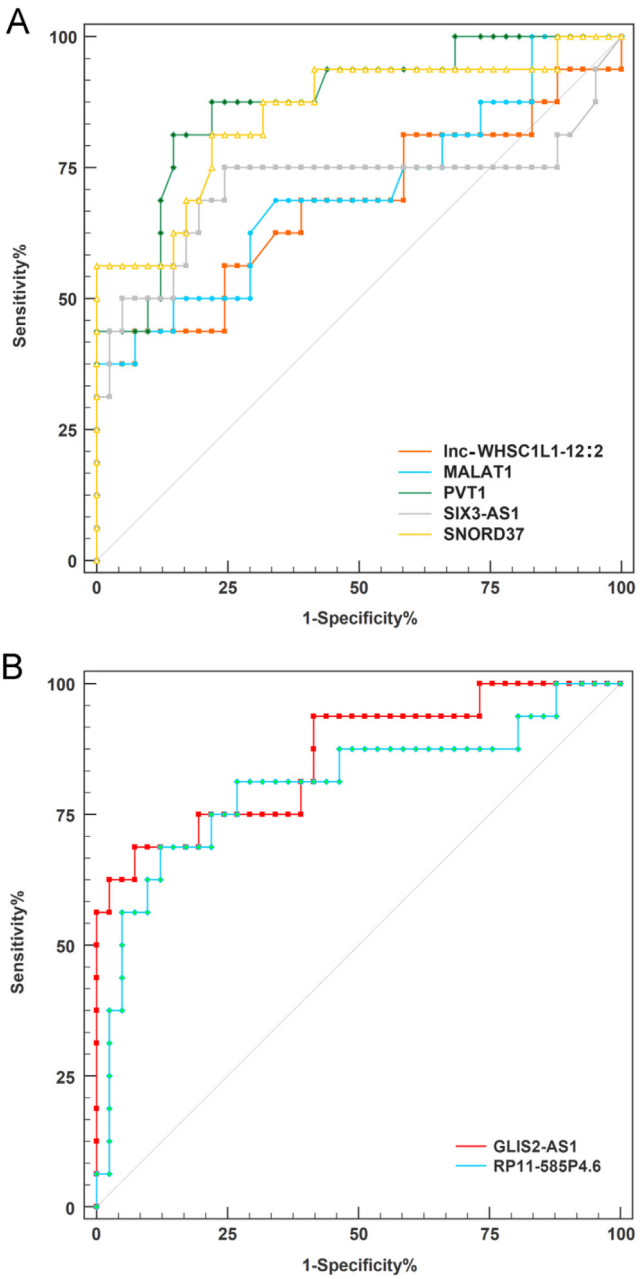

Figure 7
Diagnostic value of candidate lncRNAs assessed by ROC curve. Upregulated (A) and downregulated (B) lncRNAs that showed maximum AUC values were lncRNA PVT1 and lncRNA GLIS2-AS1. AUC, area under the curve.

PCa samples (6 samples) showed a significantly higher expression level of PVT1 (P=0.02) and lower expression level of GLIS2-AS1 (P=0.03) compared to PCa samples without *CDC73* mutation. PVT1 and GLIS2-AS1 can also discriminate *CDC73*-mutant samples in PCa, with AUC values of 0.950 and 0.933, respectively (Supplementary Table 2).

lncRNA GLIS2-AS1 and PVT1 *in situ* hybridization

The tissue expression levels of the lncRNA GLIS2-AS1 and PVT1 *in situ* were assessed and visualized in different PCa and PAd FFPE samples. Higher hybridization signals were observed in PCa for PVT1 and PAd for GLIS2-AS1 (Fig. 8).

Discussion

Accumulating evidence indicates that lncRNAs may yield abundant regulatory functions and provide different mechanisms in multiple cancer types (Klinge 2018). Studies of non-coding RNA (ncRNA) in PCa, as previously reported, have mainly focused on miRNA expression, with several differentially expressed markers identified (Verdelli & Corbetta 2017). Compared with miRNAs, lncRNAs have a more complex structure and functions linked to miRNAs, mRNAs and proteins (Thomson & Dinger 2016, Noh *et al.* 2018). Characterizing lncRNA expression profiles may provide a new understanding of parathyroid tumour origin and development. To our knowledge, this study is the first to investigate the genome-wide expression patterns of lncRNA in PCa via microarray and explore their roles in PCa.

The present study provides some clues regarding the role of mRNAs and lncRNAs in the complex molecular network of parathyroid neoplasms. Primarily, the microarray results showed that differences in lncRNA expression of PCa-PaN were substantially larger than those of PAd-PaN. Our GO and KEGG pathway analyses showed that the ECM–receptor interaction pathway was significantly altered. Interestingly, we found that several energy metabolism pathways differed between PCa and PAd. Recently, a comparative proteomic study demonstrated that mitochondrial activity might be a

Table 5 Diagnostic efficacy of candidate lncRNAs via ROC analysis.

lncRNAs	AUC	95% CI	*P*-Value
Up-regulated			
PVT1	0.871	0.768–0.975	<0.001
SNORD37	0.853	0.731–0.975	<0.001
SIX3-AS1	0.710	0.517–0.904	0.014
MALAT1	0.704	0.538–0.869	0.018
lnc-WHSC1L1-12:2	0.677	0.500–0.854	0.039
Down-regulated			
GLIS2-AS1	0.860	0.744–0.976	<0.001
RP11-585P4.6	0.805	0.660–0.949	<0.001

AUC, area under the curve; CI, confidence interval.

https://erc.bioscientifica.com
https://doi.org/10.1530/ERC-18-0480

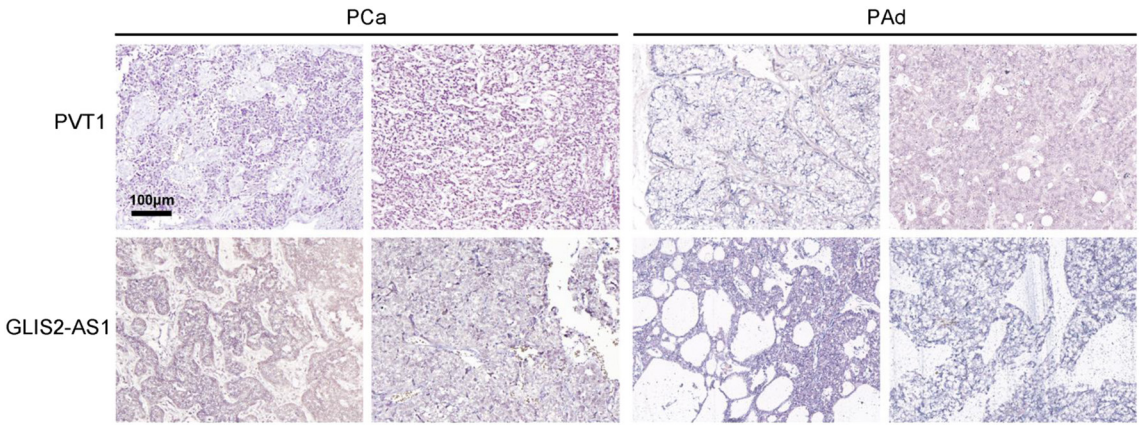

Figure 8
Representative ISH localization of lncRNA PVT1 and GLIS2-AS1 in parathyroid tumours (magnification: 200×). Representative images of lncRNA PVT1 and GLIS2-AS1 ISH signals in PCa and PAd are presented. The blue staining on FFPE tissues indicated positive ISH detection. A full colour version of this figure is available at https://doi.org/10.1530/ERC-18-0480.

potential marker for distinguishing between parathyroid hyperplasia and adenoma (Akpinar *et al.* 2017). We considered that energy metabolism changes are related to mitochondria and also occur between PAd and PCa. These molecular findings suggest that PAd and PCa should have some shared signalling and mechanisms, but exhibit more diversity than similarity. This outcome suggests that PCa has more complex mechanisms than does PAd. It is still uncertain whether PCa develops *de novo* or from PAd, but previous evidence suggests that PCa and PAd may have independent processes. STC analysis allows us to identify the sequential steps of disease by comparing gene expression from microarray data. We attempted to analyse the lncRNA and mRNA expression data in PCa and PAd tumourigenesis using STC. As a result, significant profiles were presented as 'plateau' and 'coherent' profiles. The most significant 'plateau' profile represented the components specific to carcinogenesis, and the co-expression networks showed that these transcripts had co-expression potential and biological connections. Thus, the 'plateau' pattern indicated that PAd and PCa may have independent of tumourigenesis pathways. We hypothesize that transcripts of 'coherent' profiles might be involved in certain shared process evolving from PaN to PAd or PCa, but the more dominant expression patterns indicated that PAd was not an intermediate step of PCa pathogenesis. Yet, we still lack direct evidence on this issue.

After RT-qPCR validation, selected lncRNAs in PCa were shown to have distinct expression levels compared with the PAd subset. In the PCa cohort, the lncRNA PVT1 and lncRNA GLIS2-AS1 showed optimal efficacy as diagnostic markers. lncRNA PVT1, encoded by the human *PVT1* oncogene located at 8q24.21, was also related to the *MYC* oncogene (Cui *et al.* 2016). Previous studies have demonstrated that *MYC* promotes PVT1 accumulation in cancers, and IPA analysis also revealed that *MYC* serves as a central downstream gene in the network (Tseng *et al.* 2014). On the basis of IPA, we found that core regulatory molecules ID1, FOXM1 and EZH2 were predicted to have regulatory function towards MYC. Increased MYC suggested activation of the Wnt pathway, which is involved in the epigenetic mechanisms of PCa (Pandya *et al.* 2017). In the present study, EZH2 (in profile 8) showed an important mediator role in PCa. *EZH2*, a histone methyltransferase, has been reported to show gene amplification that is common in PAd and PCa (Svedlund *et al.* 2014). Previous research has shown that lncRNA PVT1 promotes cancer cell proliferation partly by binding to *EZH2* (Wan *et al.* 2016). With coherent expression alteration in profile 13, lncRNA PVT1 has more distinct functioning patterns in PCa than PAd. Thus, the PVT1/EZH2 interaction may be indicated as a new pathogenic mechanism.

lncRNA GLIS2-AS1 (GLIS2 antisense RNA 1, chromosomal location at 16p13.3), with no available reports in cancer to date, is also in need of further study. GLIS2-AS1 was included in profile 7, which indicates that the transcript underwent a specific decrease in carcinoma. RT-qPCR results of PCa indicated that PVT1 and GLIS2-AS1 are potentially *CDC73* mutation-related lncRNAs. ISH localization indicated that PVT1 and GLIS2-AS1 can be detected and visualized in PCa and PAd tissue slides. Though we have little knowledge regarding the function of lncRNA PVT1 and GLIS2-AS1, we discovered their potential roles as a marker in various cancers, which might serve as prognostic and diagnostic indicators

(Zhu *et al*. 2017). However, larger scale validation is still needed for future clinical use. With the development of molecular technology, recent studies have focused on transcriptional profiling of parathyroid tumours using additional approaches, such as RNA-seq and nanostring chipset (Koh *et al*. 2018). Though these cancer-related molecules have not been reported in parathyroid diseases, they may be considered crucial in parathyroid oncogenesis.

Our present study has a few limitations. First, pathological diagnosis of PCa has always been difficult and sometimes subject to interobserver variability, making it prone to cause overdiagnosis or underdiagnosis (Gill 2014, Gill *et al*. 2018). Second, PCa is a rare malignancy. Tested samples may be limited, even though 16 samples were acceptable compared with previous related studies. Third, though bioinformatics analyses provide enlightening predictions for the molecular mechanism of PCa, both *in vivo* and *in vitro* experiments are needed for further verification before possible clinical applications. Forth, we also observed a high heterogeneity of the expression of selected lncRNAs and mRNAs in parathyroid tumours, indicating that the results should be validated in a larger population. Positive incidence of these candidate lncRNA markers is still unknown, which was quite important for diagnostic efficiency. In addition, the follow-up time for patients was limited, especially in some PCa cases which were free of recurrence or metastasis during follow-up.

In summary, this study explored the lncRNA and mRNA expression profiles for benign and malignant parathyroid neoplasms via lncRNA/mRNA expression microarray. Integrated analysis revealed that ECM-receptor interaction and energy metabolism pathways are differentially involved in PCa and PAd. Via RT-qPCR and ISH, the lncRNA PVT1 and GLIS2-AS1 were identified as new potential markers in differentiating PCa and PAd.

Supplementary data

This is linked to the online version of the paper at https://doi.org/10.1530/ERC-18-0480.

Declaration of interest

The authors declare that there is no conflict of interest that could be perceived as prejudicing the impartiality of the research reported.

Funding

This work was supported by the Chinese Academy of Medical Sciences (CAMS) Initiative for Innovative Medicine (CAMS-I2M) (grant number 2017-I2M-1-001) and the Peking Union Medical College Innovative Team Development Program.

Author contribution statement

Xiang Zhang, Ya Hu and Mengyi Wang conducted the experiments and analysed the data. Xiang Zhang and Ya Hu wrote and edited the manuscript. Ya Hu and Quan Liao performed the surgery. Ronghua Zhang, PeiPei Wang, Ming Cui, Zhe Su and Xiang Gao collected the tissue samples. Quan Liao and Yupei Zhao designed the study and modified the manuscript.

References

Adam MA, Untch BR & Olson JA 2010 Parathyroid carcinoma: current understanding and new insights into gene expression and intraoperative parathyroid hormone kinetics. *Oncologist* **15** 61–72. (https://doi.org/10.1634/theoncologist.2009-0185)

Akpinar G, Kasap M, Canturk NZ, Zulfigarova M, Islek EE, Guler SA, Simsek T & Canturk Z 2017 Proteomics analysis of tissue samples reveals changes in mitochondrial protein levels in parathyroid hyperplasia over adenoma. *Cancer Genomics and Proteomics* **14** 197–211. (https://doi.org/10.21873/cgp.20031)

Bartonicek N, Maag JL & Dinger ME 2016 Long noncoding RNAs in cancer: mechanisms of action and technological advancements. *Molecular Cancer* **15** 43. (https://doi.org/10.1186/s12943-016-0530-6)

Cardoso L, Stevenson M & Thakker RV 2017 Molecular genetics of syndromic and non-syndromic forms of parathyroid carcinoma. *Human Mutation* **38** 1621–1648. (https://doi.org/10.1002/humu.23337)

Costa-Guda J & Arnold A 2014 Genetic and epigenetic changes in sporadic endocrine tumors: parathyroid tumors. *Molecular and Cellular Endocrinology* **386** 46–54. (https://doi.org/10.1016/j.mce.2013.09.005)

Costa-Guda J, Imanishi Y, Palanisamy N, Kawamata N, Phillip Koeffler H, Chaganti RS & Arnold A 2013 Allelic imbalance in sporadic parathyroid carcinoma and evidence for its de novo origins. *Endocrine* **44** 489–495. (https://doi.org/10.1007/s12020-013-9903-4)

Cui M, You L, Ren X, Zhao W, Liao Q & Zhao Y 2016 Long non-coding RNA PVT1 and cancer. *Biochemical and Biophysical Research Communications* **471** 10–14. (https://doi.org/10.1016/j.bbrc.2015.12.101)

Farnebo F, Kytölä S, Teh BT, Dwight T, Wong FK, Höög A, Elvius M, Wassif WS, Thompson NW, Farnebo LO, *et al*. 1999 Alternative genetic pathways in parathyroid tumorigenesis. *Journal of Clinical Endocrinology and Metabolism* **84** 3775–3780. (https://doi.org/10.1210/jcem.84.10.6057)

Gill AJ 2014 Understanding the genetic basis of parathyroid carcinoma. *Endocrine Pathology* **25** 30–34. (https://doi.org/10.1007/s12022-013-9294-3)

Gill AJ, Lim G, Cheung V, Andrici J, Perry-Keene JL, Paik J, Sioson L, Clarkson A, Sheen A, Luxford C, *et al*. 2018 Parafibromin-deficient (HPT-JT type, CDC73 mutated) parathyroid tumors demonstrate distinctive morphologic features. *American Journal of Surgical Pathology* [epub]. (https://doi.org/10.1097/PAS.0000000000001017)

Guarnieri V, Muscarella LA, Verdelli C & Corbetta S 2018 Alterations of DNA methylation in parathyroid tumors. *Molecular and Cellular Endocrinology* **469** 60–69. (https://doi.org/10.1016/j.mce.2017.05.010)

Hu Y, Zhang X, Cui M, Su Z, Wang M, Liao Q & Zhao Y 2018 Verification of candidate microRNA markers for parathyroid carcinoma. *Endocrine* **60** 246–254 (https://doi.org/10.1007/s12020-018-1551-2)

Klinge CM 2018 Non-coding RNAs: long non-coding RNAs and microRNAs in endocrine-related cancers. *Endocrine-Related Cancer* **25** R259–R282. (https://doi.org/10.1530/ERC-17-0548)

Knoll M, Lodish HF & Sun L 2015 Long non-coding RNAs as regulators of the endocrine system. *Nature Reviews Endocrinology* **11** 151–160. (https://doi.org/10.1038/nrendo.2014.229)

Koh J, Hogue JA, Roman SA, Scheri RP, Fradin H, Corcoran DL & Sosa JA 2018 Transcriptional profiling reveals distinct classes of parathyroid tumors in PHPT. *Endocrine-Related Cancer* **25** 407–420. (https://doi.org/10.1530/ERC-17-0470)

Lloyd RV, Osamura RY, Klöppel G & Rosai J 2017 *WHO Classification of Tumours of Endocrine Organs*. *WHO/IARC Classification of Tumours*, 4th ed., vol. 10. Lyon: IARC.

Murugan AK, Munirajan AK & Alzahrani AS 2018 Long noncoding RNAs: emerging players in thyroid cancer pathogenesis. *Endocrine-Related Cancer* **25** R59–R82. (https://doi.org/10.1530/ERC-17-0188)

Noh JH, Kim KM, McClusky WG, Abdelmohsen K & Gorospe M 2018 Cytoplasmic functions of long noncoding RNAs. *Wiley Interdisciplinary Reviews: RNA* **9** e1471. (https://doi.org/10.1002/wrna.1471)

Pandya C, Uzilov AV, Bellizzi J, Lau CY, Moe AS, Strahl M, Hamou W, Newman LC, Fink MY, Antipin Y, *et al.* 2017 Genomic profiling reveals mutational landscape in parathyroid carcinomas. *JCI Insight* **2** e92061. (https://doi.org/10.1172/jci.insight.92061)

Peng R, Luo C, Guo Q, Cao J, Yang Q, Dong K, Wang S, Wang K & Song C 2018 Association analyses of genetic variants in long non-coding RNA MALAT1 with breast cancer susceptibility and mRNA expression of MALAT1 in Chinese Han population. *Gene* **642** 241–248. (https://doi.org/10.1016/j.gene.2017.11.013)

Qi P, Zhou XY & Du X 2016 Circulating long non-coding RNAs in cancer: current status and future perspectives. *Molecular Cancer* **15** 39. (https://doi.org/10.1186/s12943-016-0524-4)

Ramoni MF, Sebastiani P & Kohane IS 2002 Cluster analysis of gene expression dynamics. *PNAS* **99** 9121–9126. (https://doi.org/10.1073/pnas.132656399)

Schmitt AM & Chang HY 2016 Long noncoding RNAs in cancer pathways. *Cancer Cell* **29** 452–463. (https://doi.org/10.1016/j.ccell.2016.03.010)

Shi Y, Hogue J, Dixit D, Koh J & Olson JA 2014 Functional and genetic studies of isolated cells from parathyroid tumors reveal the complex pathogenesis of parathyroid neoplasia. *PNAS* **111** 3092–3097. (https://doi.org/10.1073/pnas.1319742111)

Silva-Figueroa AM & Perrier ND 2018 Epigenetic processes in sporadic parathyroid neoplasms. *Molecular and Cellular Endocrinology* **469** 54–59. (https://doi.org/10.1016/j.mce.2017.04.007)

Svedlund J, Koskinen Edblom S, Marquez VE, Åkerström G, Björklund P & Westin G 2012 Hypermethylated in cancer 1 (HIC1), a tumor suppressor gene epigenetically deregulated in hyperparathyroid tumors by histone H3 lysine modification. *Journal of Clinical Endocrinology and Metabolism* **97** E1307–E1315. (https://doi.org/10.1210/jc.2011-3136)

Svedlund J, Barazeghi E, Stålberg P, Hellman P, Åkerström G, Björklund P & Westin G 2014 The histone methyltransferase EZH2, an oncogene common to benign and malignant parathyroid tumors. *Endocrine-Related Cancer* **21** 231–239. (https://doi.org/10.1530/ERC-13-0497)

Thomson DW & Dinger ME 2016 Endogenous microRNA sponges: evidence and controversy. *Nature Reviews: Genetics* **17** 272–283. (https://doi.org/10.1038/nrg.2016.20)

Tseng YY, Moriarity BS, Gong W, Akiyama R, Tiwari A, Kawakami H, Ronning P, Reuland B, Guenther K, Beadnell TC, *et al.* 2014 PVT1 dependence in cancer with MYC copy-number increase. *Nature* **512** 82–86. (https://doi.org/10.1038/nature13311)

Vaira V, Elli F, Forno I, Guarnieri V, Verdelli C, Ferrero S, Scillitani A, Vicentini L, Cetani F & Mantovani G, *et al.* 2012 The microRNA cluster C19MC is deregulated in parathyroid tumours. *Journal of Molecular Endocrinology* **49** 115–124. (https://doi.org/10.1530/JME-11-0189)

Verdelli C & Corbetta S 2017 Epigenetic alterations in parathyroid cancers. *International Journal of Molecular Sciences* **18** E310. (https://doi.org/10.3390/ijms18020310)

Vogelstein B, Fearon ER, Kern SE, Hamilton SR, Preisinger AC, Nakamura Y & White R 1989 Allelotype of colorectal carcinomas. *Science* **244** 207–211. (https://doi.org/10.1126/science.2565047)

Wan L, Sun M, Liu GJ, Wei CC, Zhang EB, Kong R, Xu TP, Huang MD & Wang ZX 2016 Long noncoding RNA PVT1 promotes non-small cell lung cancer cell proliferation through epigenetically regulating LATS2 expression. *Molecular Cancer Therapeutics* **15** 1082–1094. (https://doi.org/10.1158/1535-7163.MCT-15-0707)

Wang KC & Chang HY 2011 Molecular mechanisms of long noncoding RNAs. *Molecular Cell* **43** 904–914. (https://doi.org/10.1016/j.molcel.2011.08.018)

Wang O, Wang C, Nie M, Cui Q, Guan H, Jiang Y, Li M, Xia W, Meng X & Xing X 2012 Novel HRPT2/CDC73 gene mutations and loss of expression of parafibromin in Chinese patients with clinically sporadic parathyroid carcinomas. *PLoS ONE* **7** e45567. (https://doi.org/10.1371/journal.pone.0045567)

Westin G 2016 Molecular genetics and epigenetics of nonfamilial (sporadic) parathyroid tumours. *Journal of Internal Medicine* **280** 551–558. (https://doi.org/10.1111/joim.12458)

Xue S, Chen H, Lv C, Shen X, Ding J, Liu J & Chen X 2016 Preoperative diagnosis and prognosis in 40 parathyroid carcinoma patients. *Clinical Endocrinology* **85** 29–36. (https://doi.org/10.1111/cen.13055)

Zhang K, Luo Z, Zhang Y, Zhang L, Wu L, Liu L, Yang J, Song X & Liu J 2016 Circulating lncRNA H19 in plasma as a novel biomarker for breast cancer. *Cancer Biomarkers* **17** 187–194. (https://doi.org/10.3233/CBM-160630)

Zhang D, Liu X, Wei B, Qiao G, Jiang T & Chen Z 2017 Plasma lncRNA GAS8-AS1 as a potential biomarker of papillary thyroid carcinoma in Chinese patients. *International Journal of Endocrinology* **2017** 2645904. (https://doi.org/10.1155/2017/2645904)

Zhu S, Shuai P, Yang C, Zhang Y, Zhong S, Liu X, Chen K, Ran Q, Yang H & Zhou Y 2017 Prognostic value of long non-coding RNA PVT1 as a novel biomarker in various cancers: a meta-analysis. *Oncotarget* **8** 113174–113184. (https://doi.org/10.18632/oncotarget.22830)

Received in final form 31 October 2018
Accepted 6 November 2018
Accepted Preprint published online 7 November 2018